Journal of Hydronautics

VOLUME 8 JULY 1974 NUMBER 3

Analysis of a Wave Energy Conversion Buoy

Michael E. McCormick*
U.S. Naval Academy, Annapolis, Md.

A theoretical analysis of the power generated by a pneumatic type wave-energy conversion buoy is presented. Results obtained from the analysis show that the peak-power value occurs at the resonant period of the buoy-water column system and not at the natural heaving period, as was previously assumed. A secondary peak occurs at the resonant period of the center pipe which is in free communication with the water. This resonance is similar to that of a surge chamber. The power converted by the buoy is shown to be proportional to the cube of the wave height. The length of the center pipe is shown to have an optimum value for which a maximum power is obtained at a given resonant wave period. This length corresponds to that of the water mass in the center pipe, which is approximately two-thirds of the sum of the buoy mass and the added mass.

Nomenclature

A = Eq. (22)
A_1, A_3 = area, ft^2
b = damping coefficient, lb-sec/ft
B = Eq. (22)
c = hydrostatic restoring force coefficient, lb/ft
C = added mass coefficient, Eq. (18)
f = frequency, Hz
F = force, lbs
g = gravitational acceleration, ft/sec^2
h = see Fig. 1, ft
H = wave height, ft
J_1 = Bessel function of the first order
k = wavenumber, $2\pi/\lambda$
L_1 = center-pipe length, ft
L_2 = draught of the float, ft
L_t = turbine duct length, ft
m = buoy mass, slugs
m_w = added mass, slugs
p_1, p_0 = pressure, lbs/ft^2
r_1 = center-pipe radius, ft
R = float radius, ft
s = displacement from equilibrium position, ft
t = time, sec
T = wave period, sec
V = velocity, fps
w_a = weight of air, lb
w_o = vertical velocity component of water at the center-pipe opening, fps
W = energy, ft-lb
z_b = heaving displacement, ft
α = $A_1/A_3 - 1$
γ_a = specific weight of air, lb/ft^3
γ = Eq. (24)
δ = damping coefficient in Eq. (8b), sec^2/ft
ζ = $\eta_1 - z_b$, ft
η = free-surface displacement, ft
η_1 = internal free-surface displacement
Θ = angular coordinate in the horizontal plane, radians
λ = wavelength
ξ = curvilinear flow coordinate of the air, ft
ρ = mass density, slugs/ft^3
φ = velocity potential, ft^2/sec
ω = circular frequency, 2π f, rad/sec

Subscripts

a = air
b = buoy
d = damped natural frequency
n = natural frequency of z_b-motion
N = natural frequency of ζ-motion
o = at opening of center-pipe
t = turbine duct length
w = water

Special

$\dot{W}$ = power, watts
$\bar{W}$ = time-averaged power, watts
$\bar{W}_{max}$ = maximum value of $\bar{W}$, watts
$\bar{p}$ = area-averaged pressure, lb/ft^2

Received November 30, 1973; revision received March 8, 1974. This paper was prepared for the U.S. Coast Guard, Dept. of Transportation, Washington, D.C., as Rept. EW-6-73 under Contract Z-70099-1-14050. The author wishes to express his appreciation to the U.S. Coast Guard for supporting this study. Further, a special thanks is extended to both D. Price and J. Tozzi, USCG, of the Navigation Aids Section for their advice and encouragement. Finally, the author appreciates the support and encouragement of R. D. Mathieu, Director of Research at the U.S. Naval Academy.

Index category: Marine Hydrodynamics, Vessel and Control Surface.

*Associate Professor of Ocean Engineering, Dept. of Naval Systems Engineering.

Introduction

THE goal of utilizing ocean wave energy has been a challenge to ocean engineers for many years. Various methods have been tried to capture this energy which include the use of spring-mass systems, pendulums, and pneumatic and hydraulic devices. These devices have been mounted on fixed structures, including taut-moored buoys as described in Ref. 1, to utilize the water particle motions. Floating devices, such as that described in Refs. 2 and 3, take advantage of both the water motion and the wave-induced motions of the floating body itself. The latter is of interest in the present paper.

The wave energy conversion system described in Ref. 2 is known commercially as the Wave-Activated Generator Buoy and is produced jointly by the Ryokuseisha Corporation and Kogyokaisha Limited of Japan. The principle of the buoy system can be understood by referring to the

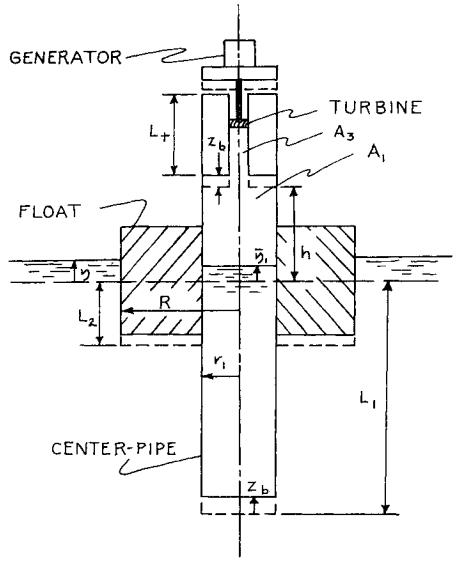

Fig. 1 Schematic of a pneumatic-type wave-energy conversion buoy.

sketch in Fig. 1. The buoy consists of a circular floatation body which contains a vertical center-pipe that has free communication with the sea. Thus, the water surface in the center of the pipe rises and falls with the same period as that of the external wave. Above the center pipe there is an area contraction through which the air above the internal free surface of the water passes. This air has a relative motion to the buoy caused by both the moving water surface and the heaving of the buoy. An air turbine is located in a small-diameter pipe which is connected to the area contraction at the top of the center pipe. This turbine is driven by the alternating air currents. The turbine, in turn, drives an electrical generator which produces energy to be used directly or stored in batteries. This type of buoy has been used successfully as a navigation aid by the Maritime Safety Agency of Japan since 1965 and is presently being used by the U.S. Coast Guard.

The purpose of this paper is to present results of a theoretical analysis of the wave energy conversion by a buoy system similar to that described in Ref. 2.

Analysis

A. Internal Air Flow Analysis

In order to analyze completely the air motion above the internal free surface which drives the turbine sketched in Fig. 1, one must account for the compressibility of the air, the viscous actions on the flow, and the unsteadiness of the flow. The mathematics involved in this analysis, therefore, become unwieldy and much of the physical significance is lost in the analysis. To simplify the analysis it is assumed that the air is incompressible and that the consequences of the viscosity can be summed in one loss term. Applying the modified unsteady energy equation between the internal free-surface and the exhaust (Fig. 1), one obtains

$$p_1/\gamma_a + \bar{V}_1^2/2g = \bar{V}_3^2/2g + \sum_i h_i + 1/g\int_{\xi_1}^{\xi_3} \partial\bar{V}/\partial t\, d\xi + dW/dw_a \quad (1)$$

where ξ is the curvilinear coordinate along the flow path, $\bar{V}$ is the area-averaged velocity at a position ξ, $\Sigma_i h_i$ is the sum of the head losses within the air passage, and dW/dw_a is the energy available to the turbine per unit weight of air. The pressure at the exhaust is assumed to be atmospheric, i.e., zero gage pressure.

Since the air is incompressible, the continuity equation can be expressed as

$$\bar{V}A = \text{constant} \quad (2)$$

where the velocity above the internal free surface is

$$\bar{V}_1 = \dot{\bar{\eta}}_1 - \dot{z}_b \equiv \dot{\zeta} \quad (3)$$

and that at the exhaust is

$$\bar{V}_3 = \dot{s}_3 - \dot{z}_b \quad (4)$$

s_3 is the displacement of the air from its equilibrium position at the exhaust and z_b is the heaving displacement of the buoy. The displacement of the internal free surface in Eq. (1) is the area-averaged value, i.e.,

$$\bar{\eta}_1 = 1/A_1\int_0^{r_1}\int_{-\pi}^{+\pi} \eta_1 r\, d\theta\, dr \quad (5)$$

where θ is the angle measured from the wave direction in the cross-sectional area of the center pipe. Similarly, the volume of air must be conserved for the incompressible flow which means that

$$(\bar{\eta}_1 - z_b)A_1 \equiv \zeta A_1 = (s_3 - z_b)A3 \quad (6)$$

The integral of the unsteady term in Eq. (1) can be evaluated by combining the integrand with the equation of continuity as expressed in Eq. (2). Relating the velocity $\bar{V}$ to $\bar{V}_1$, the integral becomes

$$\int_{\xi_1}^{\xi_3} \partial\bar{V}/\partial t\, d\xi = A_1\dot{\zeta}\int_{\xi_1}^{\xi_3} d\xi/A \quad (7a)$$

Referring to Fig. 1, the variation in area can be expressed by using the unit step function

$$u(x-a) = \begin{cases} 1, x > a \\ 0, x < a \end{cases}$$

Thus, the integrand of Eq. (7a) is

$$\frac{1}{A} = -(1/A_1)u(\xi) + (1/A_1)u(\xi - \bar{\eta}_1 + h + z_b) + (1/A_3)u(\xi)$$

The integral of Eq. (7a) is then

$$\int_{\xi_1}^{\xi_3} \partial\bar{V}/\partial t\, d\xi = (h - \bar{\eta}_1 + z_b + A_1L_t/A_3)\dot{\zeta} \quad (7b)$$

It should be noted that the expression for the area variation does not take into account the existence of the vena contracta at the area contraction; however, it is believed that this omission will not significantly affect the results obtained from the analysis.

It is assumed that the energy losses in the air flow are turbulent in nature and therefore are proportional to the square of the velocity, i. e.,

$$\sum_i h_i = \sum_i \beta_i(\dot{s}_i - \dot{z}_b)|\dot{s}_i - \dot{z}_b| \quad (8a)$$

where the absolute value is used to insure that the resistance always opposes the velocity. Further, by using the equation of continuity, Eq. (2), each loss term in the summation can be related to the air velocity adjacent to the internal free-surface. Thus, Eq. (8a) can be written as

$$\sum_i h_i = \sum_i \delta_i\dot{\zeta}|\dot{\zeta}| \quad (8b)$$

The loss coefficients δ_i depend on the type of loss experienced, e.g., contractions, bends, expansions, wall shear stress, etc.

Finally, the combination of Eqs. (1-3, 7b, and 8b) yield the following expression for the power available to the turbine:

$$dW/dt = \rho_a \dot{\zeta} \pi r_1^2 g dW/dw_a = \rho_a \dot{\zeta} \pi r_1^2 g \left\{ \frac{\bar{p}_1}{\gamma_a} - (1/2g)\alpha \dot{\zeta}^2 - \sum_i \delta_i \dot{\zeta} |\dot{\zeta}| - 1/g[h + L_t(A_1/A_3) - \zeta]\ddot{\zeta} \right\} \quad (9)$$

where

$$\alpha = (A_1/A_3)^2 - 1$$

B. Free-Surface Motions

It is assumed that the external linear waves and the associated water particle motions are unaffected by the motions of the buoy. This assumption is known as the Froude-Krylov hypothesis and is discussed by the author in Ref. 4. Assuming that the water is inviscid, the linearized Bernoulli equation can be used to obtain the pressure at the opening at the bottom of the center pipe; i.e., referring to Fig. 1, the averaged pressure over the circular opening is

$$\bar{p}_o = \frac{1}{A_1} \int_0^{r_1} \int_{-\pi}^{+\pi} p_o r d\theta dr = -\rho_w \dot{\bar{\varphi}}_o - \rho_w g(z_b - L_1) \quad (10)$$

where $\dot{\bar{\varphi}}_o$ is the area-averaged time derivative of the velocity potential at $z = z_b - L_1$. Thus, from Ref. 4, assuming deep water, the velocity potential of the right-running wave at the bottom of the center pipe is

$$\bar{\varphi} = 1/A_1 \int_o^{r_1} \int_{-\pi}^{+\pi} (Hg/2\omega) e^{-k(L_1 - z_b)} \sin(kx - \omega t) r d\theta dr = \bar{w}/ko \quad (11)$$

where H is the wave height, ω is the circular frequency, k is the wave number ($2\pi/\lambda$), and $\bar{w}_o$ is the area-averaged vertical component of the water velocity. Further, from the continuity expression,

$$\dot{\bar{\eta}}_1 = \bar{w}_o = k\bar{\varphi}_o \quad (12)$$

for the deep water wave.

Since the pressure $\bar{p}_o$ is known, the chamber pressure p_1 can be determined by applying the unsteady form of Bernoulli's equation between the lower pipe opening and the inner free surface. Thus

$$p_1 = \bar{p}_o + \rho_w g(z_b - L_1 - \bar{\eta}_1) - \rho_w(\bar{w}_o - \ddot{z}_b)(L_1 - z_b + \bar{\eta}_1) \quad (13a)$$

Since $\bar{p}_o = -\rho_w \dot{\bar{\varphi}}_o - \rho_w g(z_b - L_1)$ and, also $\ddot{\bar{\eta}}_1 = -\omega^2 \eta_1 = -kg\bar{\eta}_1$, then Eq. (13a) can be written as

$$p_1 = -\rho_w(L_1 + \zeta)\ddot{\zeta} \quad (13b)$$

C. Heaving Motions of the Buoy

The linearized heaving equation for the buoy sketched in Fig. 1 and floating in deep water is

$$(m + m_w)\ddot{z}_b + b\dot{z}_b + cz_b = F_w + F_a \quad (14)$$

where F_w is the vertical force on the floating body due to surface waves and expressed by

$$F_w = \int_A \int p_w dA + \rho_w g \int_A \int \eta dA = -\rho_w \int_{r_1}^{R} \int_{-\pi}^{+\pi} (\dot{\varphi}_w - g\eta) r d\theta dr \quad (15)$$

where p_w is the dynamic wave pressure of the linearized wave, m is the buoy mass, m_w is the added-mass of the buoy, b is the viscous and wave damping coefficient described by

$$b = \{4c(m + m_w) - 16\pi^2 f_d^2 (m + m_w)^2\}^{1/2} \quad (16)$$

f_d is the measured damped natural frequency of the heaving motion, and c is the hydrostatic restoring force defined by

$$c = \rho_w g \pi (R^2 - r_1^2) \quad (17)$$

The added mass excited by the heaving circular floatation body (see Appendix B) is

$$m_w = C\rho\pi(R - r_1)^3 \quad (18)$$

The force due to the vertical momentum of the internal air flow is

$$F_a = \rho_a A_1 \dot{\zeta}^2 + p_1 A_1 = \rho_a \pi r_1^2 \dot{\zeta}^2 - \rho_w \ddot{\zeta}(L_1 + \zeta)\pi r_1^2 \quad (19)$$

where the expression for the chamber pressure p_1 which is found in Eq. (13b) is used.

Equations (9, 13b, and 14) form a set of three equations with three functions to be determined; i.e., p_1, z_b, and dW/dt. The motion of the internal free-surface, η_1, is determined by the external sinusoidal wave.

D. Example

To obtain an idea of the magnitudes of the wave power which is made available to the turbine by the energy converting buoy, the analysis is now applied to the experimental buoy used by Y. Masuda in a fresh water wave tank and described in Ref. 3. Referring to Fig. 1 for notation, the values which approximately describe the buoy of Ref. 3 are the following:

$$\begin{aligned} A_1 &= 2.835 \text{ ft}^2 \\ A_3 &= 0.1\, A_1 \\ f_d &= 0.98\, f_n \\ H &= 1.31 \text{ ft} \\ h &= 2.5 \text{ ft} \\ L_1 &= 15 \text{ ft} \\ L_t &= 2.5 \text{ ft} \\ L_2 &= 2.267 \text{ ft} \\ m &= 82.3 \text{ slugs}, \quad m_w = 66.8 \text{ slugs} \\ R &= 2.62 \text{ ft} \\ r_1 &= 0.95 \text{ ft} \\ \rho_a &= 0.00237 \text{ slugs/ft}^3 \\ \rho_w &= 1.93 \text{ slugs/ft}^3 \\ \sum_i \delta_i &= 225 \text{ sec}^2/\text{ft} \end{aligned}$$

When the above values are used in the analysis, the nonlinear terms in the heaving equation (14) which are due to the momentum transfer of the internal air flow, Eq. (19), are negligible for the following reasons. First, the term $\rho_a \pi r_1^2 \dot{\zeta}^2$ in Eq. (19) is of second order because of the very small value of ρ_a. Secondly, for a purely heaving body in linear waves, $L_1 \gg |\zeta|$ is the second term of Eq. (19). The linearized heaving equation (14) is then

$$\begin{aligned} (m + m_w)\ddot{z}_b + b\dot{z}_b + cz_b &= -\rho_w \int_1^R \int_{-\pi}^{+\pi} \left\{ -\frac{Hg}{2} e^{-k(L_2 - z_b)} \cos[kr\cos(\theta) - \omega t] + \frac{Hg}{2} \cos[kr\cos(\theta) - \omega t] \right\} r d\theta dr - \rho_w \pi r_1^2 \ddot{\zeta} L_1 \\ &= \frac{\pi \rho_w Hg}{k}(1 - e^{-kL_2})[RJ_1(kR) - r_1 J_1(kr_1)] \cos(\omega t) - \rho_w \pi r_1^2 \ddot{\zeta} L_1 \end{aligned} \quad (20)$$

where the integration is demonstrated in Appendix B. In order to put Eq. (20) in terms of $\zeta = \bar{\eta}_1 - z_b$, subtract $(m + m_w)\ddot{\bar{\eta}}_1 + b\dot{\bar{\eta}}_1 + c\bar{\eta}_1$ from both sides of that equation, and then replace the internal free surface, $\bar{\eta}_1$, by the following:

$$\bar{\eta}_1 = \frac{Hg}{\omega^2 r_1} e^{-kL_1} J_1(kr_1) \cos(\omega t) \quad (21)$$

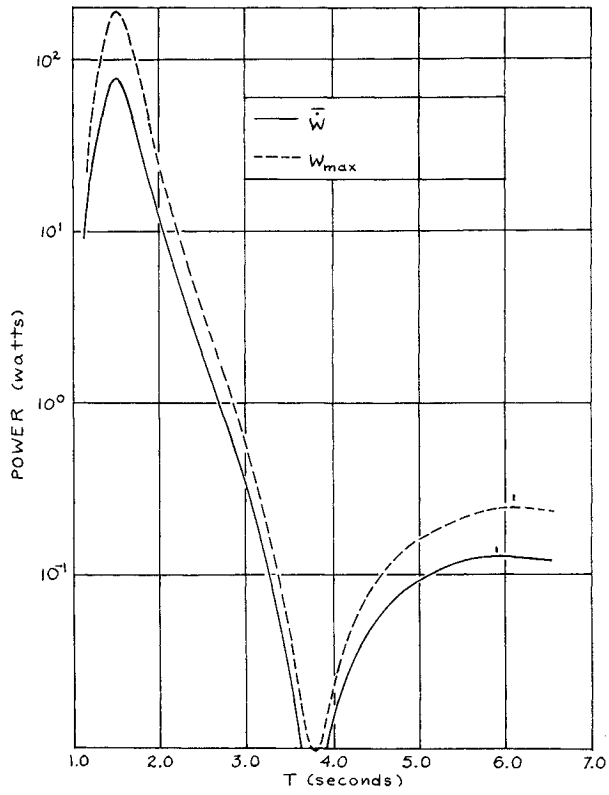

Fig. 2 Peak and time-averaged power as functions of wave period.

which is obtained from the time integration of the combination of Eq. (11) and (12). The spacial integration involved in the averaging is again given in Appendix B. In the last exponential term in Eq. (20), the term z_b is omitted. This does not introduce serious error and, furthermore, is in concert with the Froude-Krylov hypothesis mentioned in Pt. B of the Analysis. The modified and linearized heaving equation can now be written as

$$(m + m_w - \rho_w \pi r_1^2 L_1)\ddot{\zeta} + b\dot{\zeta} + c\zeta = -\frac{\pi \rho_w H g}{k}(1 - e^{-kL_2})[RJ_1(kR) - r_1 J_1(kr_1)]\cos(\omega t) - \frac{Hge^{-kL_1}}{r_1}J_1(kr_1)\left[\left(m + m_w - \frac{c}{\omega^2}\right)\cos(\omega t) + \frac{b}{\omega}\sin(\omega t)\right] = A\cos(\omega t) + B\sin(\omega t) = F_o\cos(\omega t + \gamma) \quad (22)$$

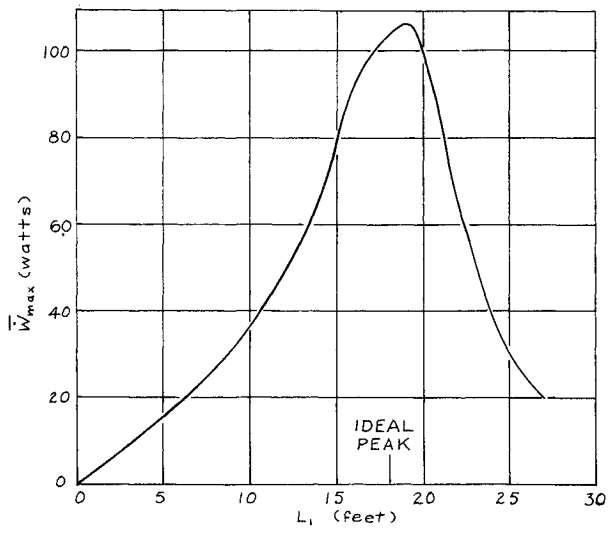

Fig. 3 Peak time-averaged power variation with center-pipe length.

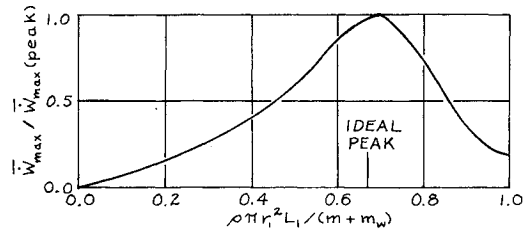

Fig. 4 Normalized peak averaged power variation with mass ratio.

where

$$F_o = (A^2 + B^2)^{1/2} \quad (23)$$

and the phase angle is

$$\gamma = \tan^{-1}(-B/A) \quad (24)$$

Following the method of Ref. 4, the solution to the modified heaving equation (22), is

$$\zeta = \frac{F_o}{c}\{(1 - \omega^2/\omega_N)^2 + (2\Delta\omega/\omega_N)^2\}^{-1/2}\cos(\omega t + \gamma - \sigma) \quad (25)$$

where

$$\sigma = \tan^{-1}\{2\Delta\omega/\omega_N/1 - (\omega/\omega_N)^2\} \quad (26)$$

$$\Delta = \frac{b}{2}\{c(m + m_w - \rho_w \pi r_1^2 L_1)\}^{-1/2} \quad (27)$$

and, finally, the natural circular frequency is

$$\omega_N = [c/(m + m_w - \rho_w \pi r_1^2 L_1)]^{1/2} \quad (28)$$

To obtain the power available to the turbine, simply combine Eqs. (25) and (13b) with Eq. (9). Results of this combination using the forementioned parametric values are presented in the next section.

Theoretical Results

The numerical values presented in Pt. D of the Analysis are used as the standard values in this section, i.e., results obtained by varying each parameter should be compared with those results obtained by using the standard values. The peak power and the time-averaged power per cycle available to the turbine are shown in Fig. 2 as functions of the wave period. The peak values for both of the curves occur at the wave period which corresponds to the damped natural frequency of the buoy-water column system. A second peak, which is somewhat obscure, occurs at a higher wave period. This period occurs at approximately the resonant frequency of the column of water in the center-pipe.

In Fig. 3 the effect of the variation of the center-pipe length L_1 on the maximum value of the time-averaged power is presented. A peak value in this power occurs when $L_1 \simeq 19$ ft. To determine the condition for this peak, a derivative with respect to L_1 of the expression in Eq. (9) is set equal to zero, while assuming the ideal situation of zero internal resistance, i.e., $\Sigma\delta_i = 0$ and $A_1 = A_3$ so that $\alpha = h = L_t = 0$. The resulting value of L_1 is 18.1 ft and, furthermore, this value is obtained when the ratio of the water-column mass to the sum of the buoy mass plus the added mass is equal to ⅔. The L_1-variation, therefore, can be attributed to the variation of the mass-ratio. The normalized maximum-averaged power is shown in Fig. 4 as a function of the mass ratio. The actual peak value occurs at a mass ratio of approximately 6.9 although, as previously mentioned, the ideal peak occurs at a value of 0.667.

The maximum time-averaged power variation with wave height is shown in Fig. 5. In this figure both the standard 15-ft center pipe and the 19-ft length are

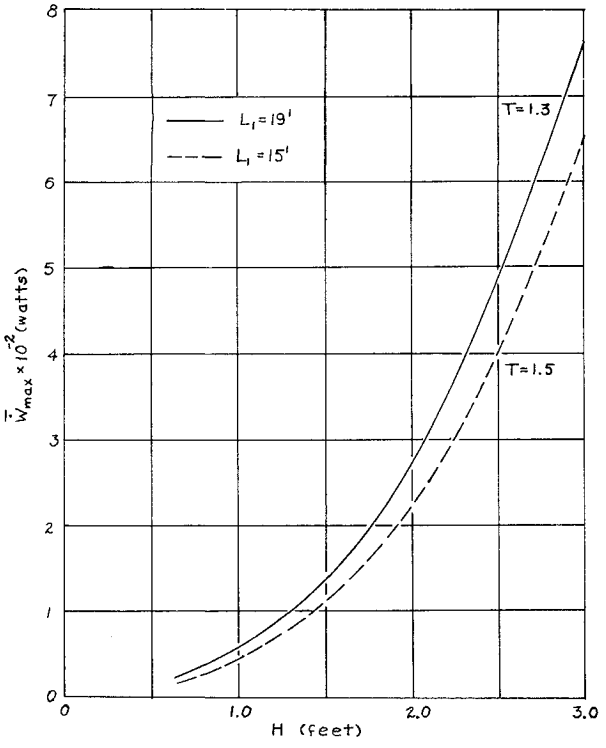

Fig. 5 Peak averaged power variation with wave height.

shown for comparison. The maximum values of $\dot{W}$ occur at different periods for these two lengths since the natural frequency of the water column and buoy system changes with length.

Finally, the actual time variations of the heaving motion, z_b, relative internal free-surface displacement ζ, chamber pressure p_1, and power $\dot{W}$ are shown in Fig. 6 for the 19-ft water column. In Fig. 6a the time-variations at the 1.3 sec wave period are shown, while those variations corresponding to a wave period of 7.0 sec are presented in Fig. 6b. These periods correspond to the two relative peaks in the time-averaged power curve for L_1 = 19 ft. These curves are similar in their phase relationships to those obtained for the 15-ft water-column buoy.

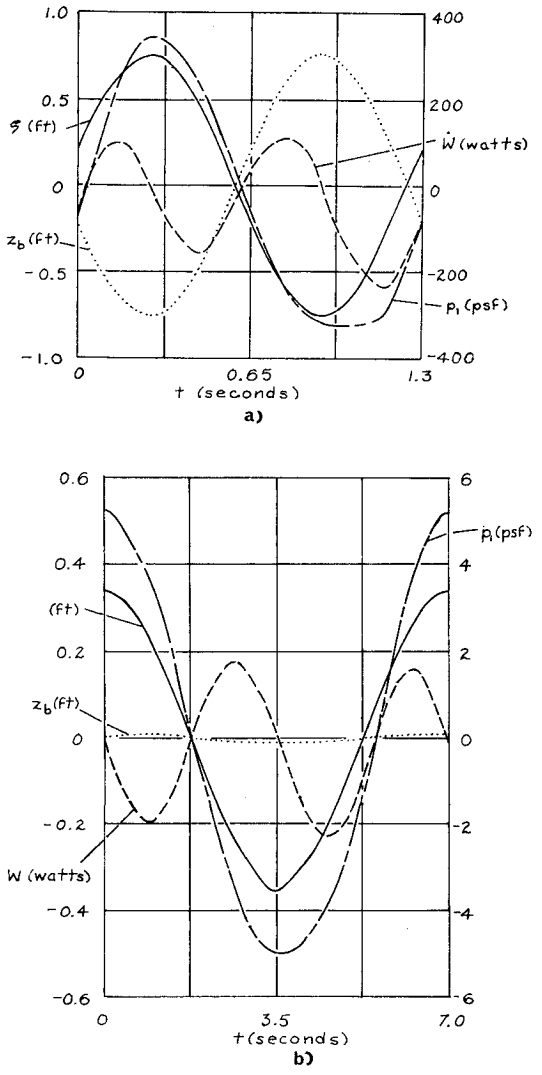

Fig. 6 a) Time-variations for L_1 = 19 ft, T = 1.3 sec. b) Time-variations for L_1 = 19 ft, T = 7.0 sec.

Discussion

As can be observed in Fig. 2, the wave-energy conversion buoy is most effective in a narrow period band about the damped natural period of the buoy-water column system. This period is obtained from the following relationship,[4]

$$f_N = \frac{\omega_N}{2\pi}(1 - \Delta^2)^{1/2} \tag{29}$$

where ω_N is given in Eq. (28) and Δ is in Eq. (27). Using the values presented in Pt. D of the Analysis, from Eq. (29) one obtains f_N = 0.667 Hz. Thus, when L_1 = 15 ft, the peak power occurs at a resonant period of 1.50 sec.

The second relative peak power value occurs at the natural period of the center-pipe. This relative peaking is due to a resonance which is similar to that of a surge tank, as described in Ref. 6. For the ideal case of no internal resistance in the center pipe, air chamber, or turbine passage, the resonant period is approximately given by the inviscid formula

$$T = 2\pi(L_1/g)^{1/2} \tag{30}$$

which for a length of 15 ft yields T = 4.29 sec. The value of the period of the second peak in Fig. 2, however, is approximately 6 sec for L_1 = 15 ft. The difference in the values is due to the air resistance as represented by $\Sigma\delta_i$ in the power equation, i.e., Eq. (9). The increase of this term and the corresponding adjustments in the area A_3 will cause the resonant period to increase from the ideal value predicted by Eq. (30).

The variation of the maximum time-averaged value with respect to the center-pipe length is contrary to the conclusion drawn in Refs. 2 and 3, i.e., that the power always increases with the length of the water column. The reason for the discrepancy is that the length values studied in the experiments of Refs. 2 and 3 were approximately 7.5 ft, 15 ft, and 21 ft. Referring to Fig. 3 one sees that the corresponding power values are, in fact, ascending. Thus, one would naturally draw the conclusion that an increase in L_1 would result in an increase in the power obtained from the waves. This is not the case since the inertial reaction of the water column is opposite to that of the buoy mass and added mass, as can be seen in Eq. (22). It should also be noted that the natural frequency of the buoy and water column system, as given by Eq. (28), increases as the mass in the water column increases, and when $m + m_w < \rho_w \pi r_1^2 L_1$ then the analysis yields an imaginary frequency. This can be physically interpreted as a nonoscillatory case since the trigonometric functions involving ωt become hyperbolic functions.

From Fig. 5 one sees that the wave height H has a most significant effect on the maximum time-averaged power values. The reason is that the power is proportional to H^3 as can be seen in the combination of Eqs. (9) and (25). It must be remembered that the energy in a wave is propor-

tional to H^2; however, the power derived from the wave is a product of the energy and fluid velocity. Thus, $\dot{W}$ is proportional to cube of the wave height.

The nature of the power conversion can be seen in Fig. 6. Figure 6a shows the temporal behavior of the power converted by the buoy with a 19-ft water column at the resonant period of the buoy and water column system, i.e., $T = 1.3$ sec. In this case the relative motion of the free surface and the chamber pressure are in phase, which is the situation for the maximum air velocity past the turbine. Further, by comparing the z_b and ζ curves it is apparent that the absolute values of these two functions are approximately equal for any time t. Thus, the internal free-surface motion is very small at the lower peak. The cause of these small values of $\dot{\bar{\eta}}$ is seen in Eq. (12). $\bar{\eta}$ depends on the wave-induced particle motions at the lower opening of the center pipe which are very small for short (low-period) waves. Thus, the power generated at the low-period peak is primarily due to the heaving motion of the buoy.

For longer waves, e.g., 251 ft for a 7 sec period, the heaving motions of the buoy are small; however, the particle motion at the bottom of the center pipe is relatively large.

Conclusions

From the results presented in this paper, the following conclusions can be drawn:

1) The wave-energy converting buoy is most effective for waves near the resonant period of the buoy and water-column system, as determined from Eq. (28).

2) The optimum design of the buoy is such that the water mass in the center pipe is approximately ⅔ of the buoy mass and the added mass combined. This statement must be considered in light of the assumptions of the theory, i.e., no compressibility effects, inviscid water flow, and linear waves with uniform energy spectra.

3) The power produced by the buoy increases proportionately to the cube of the wave height.

Appendix A: Integral of Eq. (20)

Consider the following integral:

$$I = \int_0^{r_1}\int_{-\pi}^{+\pi} \cos[kr\cos(\theta) - \omega t]r\,d\theta\,dr$$

$$= \frac{1}{2}\int_0^{r_1}\int_{-\pi}^{+\pi}[e^{-ikr\cos(\theta)\,+\,i\omega t} + e^{ikr\cos(\theta)\,-\,i\omega t}]r\,d\theta\,dr$$

From Ref. 5, the following relation is obtained:

$$J_m(x) = \frac{i^{-m}}{2\pi}\int_{-\pi}^{+\pi} e^{ix\cos(\theta)\,-\,im\theta}d\theta$$

Thus

$$I = \pi\int_0^{r_1} r_1[e^{i\omega t}J_o(-kr) + e^{-i\omega t}J_o(kr)]dr$$

$$= \frac{2\pi}{k}r_1J_1(kr_1)\cos(\omega t)$$

Appendix B: Added-Mass Calculation†

Since the geometry of the heaving body does not lend itself to a theoretical analysis of the added mass, one must rely on the experimentally determined natural frequency of the heaving body for this determination, i.e., f_N which is obtained from Eq. (28). Thus

$$f_N = \frac{1}{2\pi}\left(\frac{c}{m + m_w - \rho_w\pi r_1^2L_1}\right)^{1/2}$$

where c is the hydrostatic restoring coefficient given by Eq. (17). Solving for the added mass, one obtains

$$m_w = c/(4\pi^2f_N^2) - m + \rho_w\pi r_1^2L_1$$

To relate this quantity to the mass of a hemisphere of water of radius $(R - r_1)$, let

$$m_w = C\rho_w\pi(R - r_1)^3$$

where C is a numerical coefficient corresponding to the buoy geometry. The value of this coefficient which corresponds to the buoy of Refs. 2 and 3 is

$$C = 66.8/1.93\pi(2.62 - 0.95)^3 = 2.36$$

References

[1]Silvers, J. P., "Successful Conversion of Ocean Wave Energy," *Marine Technology Society, Buoy Technology Conference,* March 1964, pp. 279–304.

[2]Masuda, Y., "Wave Activated Generator," paper presented at the International Colloquim on the Exposition of the Oceans, March 1971, Bordeau, France.

[3]Masuda, Y., "Wave Activated Generator—Progressive Report," July 1966, Research Institute of Japan, Tokyo.

[4]McCormick, M. E., *Ocean Engineering Wave Mechanics,* Wiley, New York, 1973.

[5]Hochstadt, H., *Special Functions of Mathematical Physics,* Holt, Rinehart & Winston, New York, 1961.

[6]McNown, J. S., "Surges and Water Hammer," in *Engineering Hydraulics,* edited by H. Rouse, Wiley, New York, 1950.

†*Note:* As $r_1 \to R$, $m_w \to 0$, and as $r_1 \to 0$, $m_w \to 258$ (theoretically).